Spiking neuron models with excitatory or inhibitory synaptic couplings and synchronization phenomena

Yasuomi D. Sato and Masatoshi Shiino
Department of Applied Physics, Faculty of Science, Tokyo Institute of Technology, 2-12-1 Oh-okayama, Meguro-ku, Tokyo 152-0033, Japan
(Received 16 January 2002; published 10 October 2002)

We investigate synchronization phenomena in a system of two piecewise-linear-type model neurons with excitatory or inhibitory synaptic couplings. Employing the phase plane analysis and a singular perturbation approach to split the dynamics into slow and fast ones, we construct analytically the Poincaré map of the solution to the piecewise-linear equations. We investigate conditions for the occurrence of synchronized oscillations of in phase as well as of antiphase in terms of parameters representing the strength of the synaptic coupling and the decaying relaxation rate of the synaptic dynamics. We present the results of numerical simulations that agree with our theoretical ones.

DOI: 10.1103/PhysRevE.66.041903 PACS number(s): 87.10.+e, 02.60.Cb, 05.45.Xt

I. INTRODUCTION

Synchronous firing of neurons that has been observed in the cat visual cortex has attracted much attention from researchers [1–4]. In order to understand highly integrated neural information processing in physiological nervous systems, theoretical studies of synchronization phenomena in neuronal networks have been extensively undertaken [5–8]. Synchronized oscillations exhibited by coupled oscillator systems are one example of cooperative phenomena. Their dynamic behavior is becoming an active area of statistical mechanics of nonequilibrium phase transitions. Various kinds of coupled oscillators ranging from theoretically tractable models to physiologically relevant ones and from small size populations to large size ones have been proposed and extensively studied.

In physiologically relevant oscillator models, either or both of the oscillators whose components and couplings between them are made realistic in some sense. A unit component may take the form of an oscillator that is made as simple as possible like the integrate-and-fire-type oscillator or the FitzHugh-Nagumo (FHN)-type oscillator, while in a more realistic model, an oscillator based on the Hodgkin-Huxley (HH) equations or multicompartment model can be conveniently used to explain the result of any physiological experiments.

For couplings between oscillators, one can consider two types of couplings found in the real nervous system: the chemical synapse and the electrical synapse.

Electrical synapses [9–11] are diffusive-type couplings and have linear membrane potentials, whereas chemical synapses contain nonlinear couplings. The latter have been more often used than the former, a fact that has recently begun to attract attention as a possible mechanism for synchronized oscillations in the inhibitory interconnected network.

Modeling of chemical synapses, which are classified into excitatory and inhibitory ones, may include either the dynamics representing a certain chemical gating kinetics or the so-called α function. One of the key issues of synchronization phenomena exhibited by coupled oscillators with the above-mentioned chemical synapses will be the relationship between the types of entrainment of oscillations and synapses together with synchronization-desynchronization transitions.

Many computer simulation experiments conducted previously have demonstrated that neuronal ensembles become asynchronized and synchronized by mutual excitation and mutual inhibition, respectively [12–15]. A theoretical study based on the two integrate-and-fire oscillator models and on two phase oscillator models with synaptic coupling having the α function, has given an explanation of how the synaptic time constant governs the stability of phase-locked solutions. It was confirmed that inhibitory synchronization and excitatory asynchronization occur when the synaptic relaxation rate is large [16].

The study based on simulations of either two or more synaptically interconnected neurons has extensively been conducted to explore the collective behavior. Systematic exploration of the parameter space of model dynamics, however, has been lacking. We consider that the study of two coupled neurons can still yield a useful insight into the synchronization phenomena found in larger neural networks [17–21].

The aim of this paper is to study an exactly solvable model of a system of two coupled neurons from the view point of finding how the static as well as dynamic properties of synaptic couplings affect the scheme of synchronization of oscillations.

We use the two interconnected neural oscillators of the piecewise linear type with excitatory or inhibitory synaptic couplings [22,23]. Moreover, we note the so-called two-time-scale motion that arises from the fact that a neuron's impulse consists of fast and slow motions. This idea allows us to employ the singular perturbation approach [24–27] to split the dynamics into slow and fast ones [28–33]. We then ignore the fast dynamics and give attention only to the slow ones as we let the time-scale parameter approach 0. For the modeling of the synaptic couplings, we incorporate first-order kinetics of the gating variable for inactivation instead of employing the α-function.

We make full use of the Poincaré map of the solutions to the piecewise-linear equations, which is constructed analytically, for example, by considering the state of two neurons that occur immediately after one of them fires as the iterated points in the Poincare surface. Such a map enables us to investigate conditions for the occurrence of synchronized oscillations of the in phase (0 phase lag) as well as the antiphase ($|W_1-W_2|\approx 0.5$), in terms of the parameters of the synaptic coupling. In the case of excitatory coupling, if the decaying relaxation rate is large, two neurons become synchronized in the in phases or antiphases, depending on the initial conditions. However, when the rate is small, they become synchronized in the in phase. In the case of inhibitory coupling, two neurons become synchronized in the antiphases or quasiantiphases, depending on the decaying relaxation rate. We summarize the result by drawing a phase diagram of the parameter space of the strength and the decaying relaxation rate of the synaptic couplings and compare this result with numerical simulations. The simulations are conducted using the fourth-order Runge-Kutta method for the HH, the FHN, and the piecewise-linear models.

The outline of the paper is as follows. In Sec. II, the coupled FHN model with a piecewise-linear approximation is presented together with the model of synaptic kinetics. The separation between the slow dynamics and the fast ones is made by introducing the time-scale parameter. We then obtain three fundamental types of solutions for the time evolutions of the two coupled neurons in the limit that the time-scale parameter tends to 0. In Sec. III, using the three types of solutions, we construct one- or two-dimensional Poincaré maps under the assumption that the in phase or antiphase synchronized solutions exist. In the case of excitatory couplings, we use a one-dimensional map for in-phase synchronization and conduct the linear stability analysis. In Sec. IV, we present the results of numerical simulations that agree with those of our analysis. We give a summary and brief discussions in Sec. V.

II. MODEL BASED ON THE FHN TYPE NEURONS WITH THE PIECEWISE-LINEAR APPROXIMATION

We begin by describing two interconnected neural oscillators of the piecewise-linear type with excitatory or inhibitory synaptic couplings,

$$\frac{dV_i}{dt} = -cV_i + |V_i+1| - |V_i-1| - W_i + I_{syn}^{(i)}, \qquad (1)$$

$$\frac{dW_i}{dt} = \epsilon(V_i + a - bW_i) \quad (i=1,2), \qquad (2)$$

where a, b, and c are constant, $I_{syn}^{(i)}$ represents the synaptic coupling, and $\epsilon(>0)$ is a small time-scale parameter. We assume $0<c<2$, $-1<a/[b(2-c)-1]<1$ and $2-c<1/b$ so that the model represents an oscillatory system exhibiting a spontaneous and periodic firing. V is the excitable variable describing something similar to an action potential. W is the recovery variable and is like the total ionic channel in the HH model. It is often convenient to use the phase plane

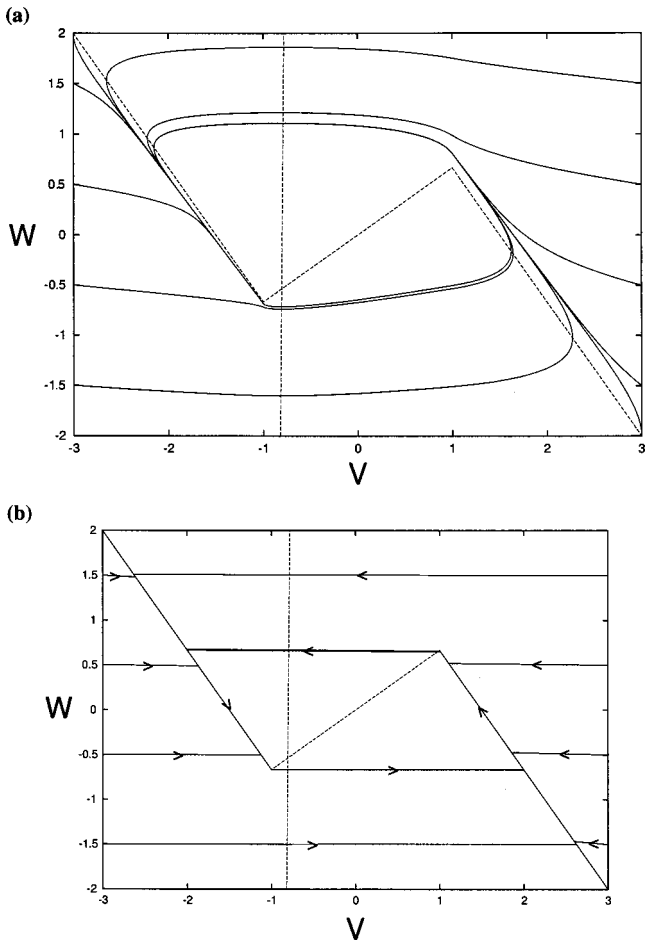

FIG. 1. Phase plane of the piecewise-linear model. (a) $\epsilon=0.1$. (b) $\epsilon\to 0$. The solid lines indicate dynamical flow. The broken lines present the nullclines, that is, $\dot{V}=0$ and $\dot{W}=0$. Here we set $a=0.8$, $b=0.01$, and $c=4/3$.

(V,W) representing time evolution of (V,W) as shown in Fig. 1(a), where V has the inverted N-shaped nullcline and W has the one that is a straight line with a positive slope. We also call the flow around the left branch the silent, or inactive phase and its right branch, the active phase. We call the local minima of the V nullcline the left knee point and its local maxima the right knee point. The reason for introducing the time-scale parameter ϵ will be explained later.

For the synaptic coupling $I_{syn}^{(i)}$, we incorporate the first-order kinetics instead of using the α function, to write

$$I_{syn}^{(i)} = G_{syn} s_{\bar{i}}, \qquad (3)$$

where $\bar{i}$ represents the counterpart of neuron i and G_{syn} the synaptic strength. It represents an excitatory coupling when $0<G_{syn}<[(1+a)/b]-(2-c)$, and an inhibitory one when $[(-1+a)/b]+(2-c)<G_{syn}<0$. We consider that s_j obeys the following equation:

$$\frac{ds_j}{dt} = \alpha F(V_j)(1-s_j) - \epsilon\beta s_j,$$

$$F(V_j)=\frac{1}{1+\exp\left(-\dfrac{V_j-\theta}{\sigma}\right)} \quad (j=1,2), \tag{4}$$

where $F(V)$ is the sigmoid function with threshold θ and small σ, and α and β represent the synaptic rising and decaying relaxation rates, respectively.

To split the slow dynamics from the fast ones, we rewrite the piecewise-linear model by changing the time scale to $\tau=\epsilon t$:

$$\epsilon\frac{dV_i}{d\tau}=-cV_i+|V_i+1|-|V_i-1|-W_i+G_{syn}s_i^-, \tag{5}$$

$$\frac{dW_i}{d\tau}=V_i+a-bW_i, \tag{6}$$

$$\epsilon\frac{ds_i}{d\tau}=\begin{cases}\alpha(1-s_i)-\epsilon\beta s_i & (V_i>\theta),\\ -\epsilon\beta s_i & (V_i<\theta).\end{cases} \tag{7}$$

As ϵ becomes smaller, the motions in the active and silent phases become slower, while the switching ones between them become faster and its trajectory on the V-W plane roughly follows a line of constant W_i.

Then, taking the limit $\epsilon\to 0$, one obtains a simplified model where transitions between the silent and active phases become instantaneous. In other words, for V_i, and s_i when $V_i>\theta$, it suffices to consider the manifold obtained by setting $dV_i/d\tau=0$, and $ds_i/d\tau=0$

$$0=-cV_i+|V_i+1|-|V_i-1|-W_i+G_{syn}s_i^-, \tag{8}$$

$$\frac{dW_i}{d\tau}=V_i+a-bW_i, \tag{9}$$

$$\frac{ds_i}{d\tau}=\begin{cases}0\to s_i=1 & (V_i>\theta),\\ -\beta s_i & (V_i<\theta).\end{cases} \tag{10}$$

These equations are the simplified version of the piecewise-linear model. They ignore the switching motions between the active and silent phases and give attention only to the active and silent phases. We depict Fig. 1(b) to show that a trajectory follows a straight line of constant W_i to enter the active and silent phases after arriving at the left and right knee points, respectively. In both Figs. 1(a) and 1(b), it can be noted that the transition $\epsilon\to 0$ leaves the structure of the phase space intact.

We proceed to solve Eqs. (8)–(10). In solving these equations, we have to consider the following three fundamental cases according to whether neurons i and j are firing or not. Here we consider the solutions in the case of $\beta\neq b+(1/c)$. The case of $\beta=b+(1/c)$ is also satisfied by the following analysis.

Case (1). Both the two neurons $i(=1,2)$ are firing in the active phase

$$W_i^{++}(\tau)=[W_i^{++}(\tau_0)-D_+]e^{-[b+(1/c)](\tau-\tau_0)}+D_+, \tag{11}$$

$$s_i^+(\tau)=1. \tag{12}$$

Case (2). Neuron i is not firing in the silent phase, while neuron j is firing in the active one $(i,j=1,2)$

$$W_i^{-+}(\tau)=[W_i^{-+}(\tau_0)-D_-]e^{-[b+(1/c)](\tau-\tau_0)}+D_-, \tag{13}$$

$$\begin{aligned}W_j^{+-}(\tau)=&W_j^{+-}(\tau_0)e^{-[b+(1/c)](\tau-\tau_0)}\\&+A_+(1-e^{-[b+(1/c)](\tau-\tau_0)})\\&+Bs_i^-(\tau_0)(e^{-\beta(\tau-\tau_0)}-e^{-[b+(1/c)](\tau-\tau_0)}),\end{aligned} \tag{14}$$

$$s_i^-(\tau)=s_j^-(\tau_0)e^{-\beta(\tau-\tau_0)}, \tag{15}$$

$$s_j^+(\tau)=1. \tag{16}$$

Case (3). Both two neurons $i(=1,2)$ are not firing in the silent phase

$$\begin{aligned}W_i^{--}(\tau)=&W_i^{--}(\tau_0)e^{-[b+(1/c)](\tau-\tau_0)}\\&+A_-(1-e^{-[b+(1/c)](\tau-\tau_0)})\\&+Bs_j^-(\tau_0)(e^{-\beta(\tau-\tau_0)}-e^{-[b+(1/c)](\tau-\tau_0)}),\end{aligned} \tag{17}$$

$$s_i^-(\tau)=s_i^-(\tau_0)e^{-\beta(\tau-\tau_0)}, \tag{18}$$

$$D_\pm=\frac{a+\dfrac{\pm 2+G_{syn}}{c}}{b+\dfrac{1}{c}},$$

$$A_\pm=\frac{a\pm\dfrac{2}{c}}{b+\dfrac{1}{c}}, \quad B=\frac{C}{b+\dfrac{1}{c}-\beta}, \quad C=\frac{G_{syn}}{c}.$$

The above solutions allow us to analyze and understand synchronization phenomena in our present model, that is, (1), (2), and (4), in the limit $\epsilon\to 0$.

III. ANALYSIS USING THE POINCARÉ MAP

To systematically understand the behavior of the dynamics of the two coupled neurons, we analytically construct the Poincaré map corresponding to the time evolution of the system with the use of the three fundamental types of solutions, Eqs. (11)–(18). To this end, it is convenient to specify a temporal firing pattern diagram that represents how each neuron switches between the active and silent phases. According to the features of the temporal firing pattern diagram, we can construct one- or two-dimensional Poincaré maps. They enable us to gain some solutions exhibiting synchronization phenomena in the two neurons with excitatory or inhibitory synaptic couplings.

A. In-phase synchronization

We begin by investigating the case of an excitatory coupling. This case will allow the in-phase synchronization of the firing of two neurons and enable us to examine the one-dimensional Poincaré map for the analysis of such synchronization behavior.

We construct the Poincaré map by focusing on the states of two neurons that occur immediately after neuron 1's entering the silent phase with neuron 2 remaining in the active phase. Let $W_1^{(n)}$, $W_2^{(n)}$, $s_1^{(n)}$, and $s_2^{(n)}$ denote the values of W_i and s_i for the nth occurrence of such states.The Poincaré map can be defined as a map from $W_2^{(n)}$ to $W_2^{(n+1)}$. We then support that

$$W_1^{++}(0)=W_1^{-+}(0)\equiv W_1^{(n)}+G_{syn}s_2^{(n)},$$

$$W_2^{++}(0)=W_2^{+-}(0)\equiv W_2^{(n)},$$

$$s_1^{+}(0)=s_1^{-}(0)\equiv s_1^{(n)},$$

$$s_2^{+}(0)\equiv s_2^{(n)},$$

where time 0 is set to be the one when neuron 1 stops firing to enter the silent phase and hence the initial state of neurons 1 and 2 is $W_1^{(n)}=2-c$ and $s_1^{(n)}=s_2^{(n)}=1$. The Poincaré surface in this case corresponds to the surface denoted by $f(W_1,V_1)=0$, $W_1=2-c+G_{syn}$, and $s_1=s_2=1$, where $f(W,V)$ is a function of the active phase of the V nullcline of neuron 1.

Suppose that during time interval $[0,\Delta_1]$, neuron 1 is in the silent phase while neuron 2 remains in the active phase and also that at $t=\Delta_1$, neuron 2 stops firing to enter the inactive phase. Then, using case (2) in the Sec. II, the state of the two neurons at $t=\Delta_1$ is denoted by

$$W_1^{-+}(\Delta_1)=W_1^{--}(\Delta_1)=[W_1^{-+}(0)-D_-]\times e^{-[b+(1/c)]\Delta_1}+D_-, \tag{19}$$

$$W_2^{+-}(\Delta_1)=W_2^{+-}(0)e^{-[b+(1/c)]\Delta_1}+A_+[1-e^{-[b+(1/c)]\Delta_1}]+Bs_1^{-}(0)(e^{-\beta\Delta_1}-e^{-[b+(1/c)]\Delta_1}), \tag{20}$$

$$s_1^{-}(\Delta_1)=s_1^{-}(0)e^{-\beta\Delta_1}, \tag{21}$$

$$s_2^{+}(\Delta_1)=s_2^{-}(\Delta_1)=1. \tag{22}$$

When neuron 2 stops firing, we also obtain the state of two neurons as

$$W_2^{+-}(\Delta_1)=W_2^{--}(\Delta_1)=(2-c)+G_{syn}. \tag{23}$$

We know the value of Δ_1 by comparing Eqs. (20) and (23) as the solution of $Q_1(\Delta_1)=0$, where

$$Q_1(\Delta_1)=[(2-c)-A_+]+(G_{syn}-B)s_1^{-}(0)e^{-\beta\Delta_1}-[W_2^{+-}(0)-A_+-B]e^{-[b+(1/c)]\Delta_1}=0. \tag{24}$$

Similarly, suppose that for $[\Delta_1,\Delta_1+\Delta_2]$, neurons 1 and 2 are silent. At $t=\Delta_1+\Delta_2$, using case (3), the state of the two neurons is denoted by

$$W_1^{--}(\Delta_1+\Delta_2)=W_1^{--}(\Delta_1)e^{-[b+(1/c)]\Delta_2}+A_-(1-e^{-[b+(1/c)]\Delta_2})+Bs_2^{-}(\Delta_1)\times(e^{-\beta\Delta_2}-e^{-[b+(1/c)]\Delta_2}), \tag{25}$$

$$W_2^{--}(\Delta_1+\Delta_2)=W_2^{--}(\Delta_1)e^{-[b+(1/c)]\Delta_2}+A_-(1-e^{-[b+(1/c)]\Delta_2})+Bs_1^{-}(\Delta_1)\times(e^{-\beta\Delta_2}-e^{-[b+(1/c)]\Delta_2}), \tag{26}$$

$$s_1^{-}(\Delta_1+\Delta_2)=s_1^{-}(\Delta_1)e^{-\beta\Delta_2}, \tag{27}$$

$$s_2^{-}(\Delta_1+\Delta_2)=s_2^{-}(\Delta_1)e^{-\beta\Delta_2}. \tag{28}$$

Here we consider the case where neuron 2 arrives at the left knee point earlier than neuron 1. The conditions for the occurrence of this case can be specified in terms of G_{syn} and β as is shown in Appendix A. Such (G_{syn},β) region [i.e., (I)] in the G_{syn}-β plane is displayed in Fig. 2(a). We then obtain

$$W_2^{--}(\Delta_1+\Delta_2)=-(2-c)+G_{syn}s_1(\Delta_1)e^{-\beta\Delta_2}. \tag{29}$$

Moreover, as both the two neurons start firing to enter the active phase, the state of the two neurons is changed as follows:

$$W_1^{--}(\Delta_1+\Delta_2)=W_1^{++}(\Delta_1+\Delta_2),$$

$$W_2^{--}(\Delta_1+\Delta_2)=W_2^{++}(\Delta_1+\Delta_2),$$

$$s_1^{-}(\Delta_1+\Delta_2)\rightarrow s_1^{+}(\Delta_1+\Delta_2)=1,$$

$$s_2^{-}(\Delta_1+\Delta_2)\rightarrow s_2^{+}(\Delta_1+\Delta_2)=1,$$

where we have considered the case that W value of neuron 1 is larger than the value of the left knee point of V nullcline of neuron 1:

$$W_1^{--}(\Delta_1+\Delta_2)>W_2^{--}(\Delta_1+\Delta_2). \tag{30}$$

As analyzed in Appendix B, (G_{syn},β) in the region (I) of the parameter space of Fig. 2(a) ensures the above-mentioned case.

Here we explain the reason why the two neurons can simultaneously fire. In the phase plane analysis, the V nullcline of neuron 1 is shifted upward by receiving an excitatory input from neuron 2. Then the state of neuron 1, (V_1,W_1), can come below the local minima of the upward-shifted V nullcline. Therefore it is forced to start entering the right branch of the new nullcline.

Then we get the time duration Δ_2 of neuron 2 staying in the inactive phase by comparing Eqs. (25) and (29)

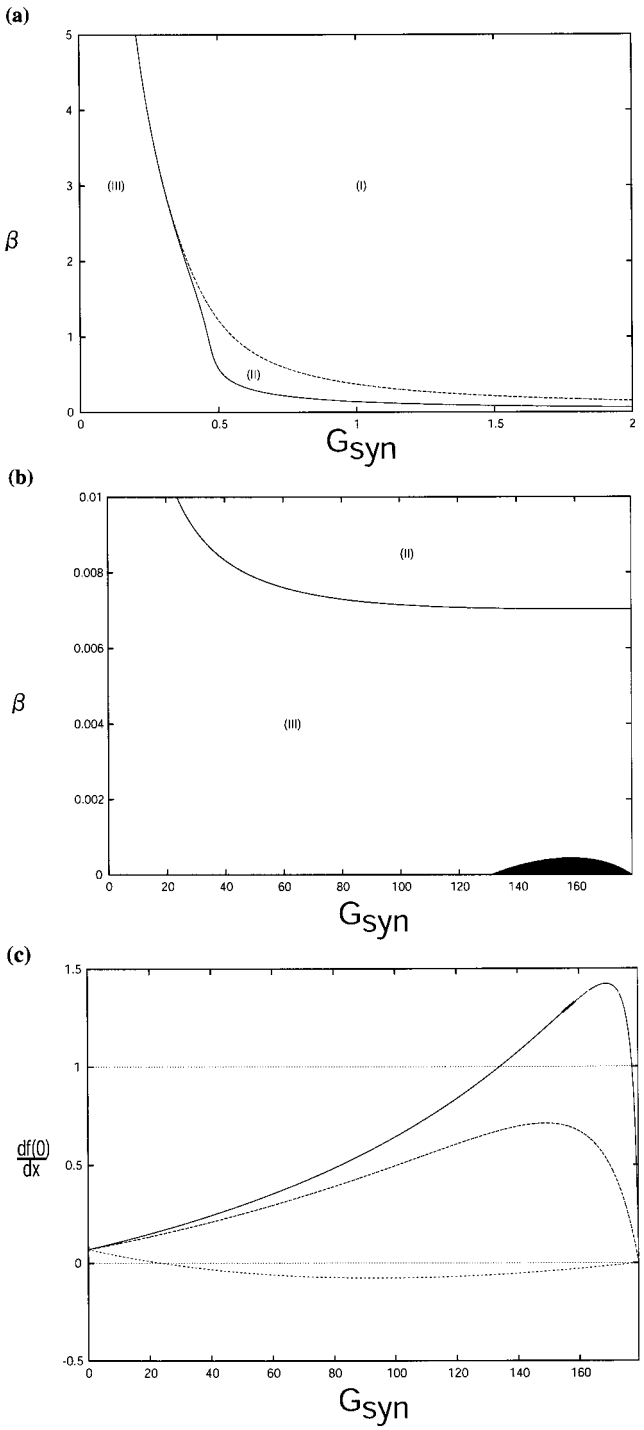

FIG. 2. Phase diagrams about in-phase synchronization with excitatory coupling. (a) G_{syn}-β diagram with respect to a firing order and a firing configuration. (b) (a)-extended diagram shows a firing order and a stability of in-phase solution. (c) G_{syn}-$(dF^{(\mathrm{III})}/dx)|_{x=0}$ diagram of the stability of the in-phase solution. The solid, dotted, and broken lines are shown when $\beta=0.001$, 0.01, and 0.1, respectively.

$$Q_2(\Delta_2)=[-(2-c)-A_-]+(G_{syn}-B)s_1^-(\Delta_1)e^{-\beta\Delta_2} -[W_2^{--}(\Delta_1)-A_--Bs_1^-(\Delta_1)]e^{-[b+(1/c)]\Delta_2}=0. \tag{31}$$

Suppose that for $[\Delta_1+\Delta_2,\Delta_1+\Delta_2+\Delta_3]$, both the two neurons are in the active phase and that at $t=\Delta_1+\Delta_2+\Delta_3$, neuron 1 stops firing. Then, making use of case (1), the state of two neurons is given by

$$W_1^{++}(\Delta_1+\Delta_2+\Delta_3)=[W_1^{++}(\Delta_1+\Delta_2)-D_+] \times e^{-[b+(1/c)]\Delta_3}+D_+, \tag{32}$$

$$W_2^{++}(\Delta_1+\Delta_2+\Delta_3)=W_2^{+-}(\Delta_1+\Delta_2+\Delta_3) =[W_2^{++}(\Delta_1+\Delta_2)-D_+] \times e^{-[b+(1/c)]\Delta_3}+D_+, \tag{33}$$

$$s_1^+(\Delta_1+\Delta_2+\Delta_3)=s_1^-(\Delta_1+\Delta_2+\Delta_3)=1, \tag{34}$$

$$s_2^+(\Delta_1+\Delta_2+\Delta_3)=1. \tag{35}$$

Neuron 1 should be at the right knee point of the upward-shifted V nullcline when it finishes firing. We then obtain $W_1(\Delta_1+\Delta_2+\Delta_3)$ as

$$W_1^{++}(\Delta_1+\Delta_2+\Delta_3)=W_1^{-+}(\Delta_1+\Delta_2+\Delta_3)=(2-c)+G_{syn}. \tag{36}$$

We also obtain the duration of neuron 1's action potential Δ_3 by comparing Eqs. (32) and (36),

$$\Delta_3=-\frac{1}{b+\frac{1}{c}}\ln\frac{(2-c)+G_{syn}-D_+}{W_1^{++}(\Delta_1+\Delta_2)+G_{syn}-D_+}. \tag{37}$$

Note that Eq. (33), which implicitly involves $W_2^{(n)}$, represents the state of neuron 2 when neuron 1 stops firing again. We arrive at the $(n+1)$th iterate of the Poincaré map.

We now obtain the explicit expression for the one-dimensional Poincaré map in terms of $W_2^{(n)}$,

$$K(W_2^{(n)})=W_2^{(n+1)}=W_2^{+-}(\Delta_1+\Delta_2+\Delta_3). \tag{38}$$

It is convenient to define the phase difference at nth iterate between two neurons as

$$x_n\equiv(2-c)+G_{syn}-W_2^{(n)} \quad (x_n\geqslant 0). \tag{39}$$

From Eq. (38), we straightforwardly obtain a one-dimensional return map for the phase difference at $(n+1)$th iterate

$$F^{(\mathrm{I})}(x)=(2-c)+G_{syn}-K[(2-c)+G_{syn}-x_n] \quad (x_n\geqslant 0). \tag{40}$$

This return map can be used in a wide region of the parameter space of G_{syn} and β. To be more precise, as far as the case with $x_n\ll 1$ is concerned, Eq. (40) is valid for (G_{syn},β) in the region (I) of G_{syn}-β plane [Fig. 2(a)]. This is because the condition Eq. (30) assumed in obtaining Eq. (40) can be shown to hold for the region (I) of Fig. 2(a) in the case with

$x_n \ll 1$ (see Appendix A). We have two other return maps for regions (II) and (III) of the G_{syn}-β plane of Fig. 2(a). They are studied in Appendix B.

We now investigate the map $x_{n+1}=F^{(\mathrm{I})}(x_n)$. Note that $x=0$ is a fixed point solution of $x_{n+1}=F^{(\mathrm{I})}(x_n)$ and gives rise to the in-phase synchronization of the two neurons. Stability of this solution is examined by the linear stability analysis,

$$\left.\frac{dF^{(\mathrm{I})}}{dx}\right|_{x=0} = -\frac{1}{-\beta(B-G_{syn})-\left(b+\frac{1}{c}\right)[(2-c)+G_{syn}-A_+-B]} \times \frac{(2-c)+G_{syn}-D_+}{[(2-c)+(G_{syn}-B)-A_-]e^{-[b+(1/c)]T_2}+Be^{-\beta T_2}+A_--D_+} \times \left[\left(b+\frac{1}{c}\right)[(2-c)+G_{syn}-D_-]e^{-[b+(1/c)]T_2}-\beta[(G_{syn}-B)e^{-[b+(1/c)]T_2}+Be^{-\beta T_2}]\right]. \tag{41}$$

This equation can also be obtained by a more intuitive manner as given in Appendix B. Stability condition is given by $0 \leqslant dF^{(\mathrm{I})}/dx|_{x=0} < 1$. For any (G_{syn},β) in region (I) of Fig. 2(a), we find that the above condition is satisfied and that the in-phase synchronized solution is stable. It is noted that for (G_{syn},β) in region (I), the approach to the $x=0$ solution is monotonic with time. The return map for region (II) can be obtained in a similar manner as the above for region (I). The only difference comes from the fact that neuron 1 arrives at the left knee earlier than neuron 2, to jump up the active phase. However, the same inequality $W_1^{--}(\Delta_1+\Delta_2) > W_2^{--}(\Delta_1+\Delta_2)$ that region (I) holds implies that neuron 1 jumps down to the inactive phase earlier than neuron 2. Thus, monotonic approach to $x=0$ can also follow. We then omit the analysis because the stability of $x=0$ can be checked by numerical simulation. Finally, we study the return map for the region (III). In the case of region (III), $W_1^{--}(\Delta_1+\Delta_2) < W_2^{--}(\Delta_1+\Delta_2)$ when both the two neurons jump up from the inactive phase to the active one. We define the phase difference at $(n+1)$th iterate as $y_{n+1}=W_2^{(n+1)}-W_1^{(n+1)}$ (>0) at the time that neuron 2 reaches the right knee point of the upward-shifted V nullcline. Hence we have the map $y_{n+1}=F^{(\mathrm{III})}(x_n)$. Iterating this map once more, we have the map from x_n to x_{n+2},

$$x_{n+2}=F^{(\mathrm{III})}(y_{n+1})=F^{(\mathrm{III})}\circ F^{(\mathrm{III})}(x_n). \tag{42}$$

Since $x=0$ is a fixed point of the map, its stability is determined by

$$\left.\frac{dF^{(\mathrm{III})}\bigcirc F^{(\mathrm{III})}(x)}{dx}\right|_{x=0} = \left.\frac{dF^{(\mathrm{III})}[F^{(\mathrm{III})}(x)]}{dF^{(\mathrm{III})}(x)}\right|_{F^{(\mathrm{III})}(x)=0} \times \left.\frac{dF^{(\mathrm{III})}(x)}{dx}\right|_{x=0} = \left[\frac{dF^{(\mathrm{III})}(0)}{dx}\right]^2 < 1, \tag{43}$$

where we easily find the following equation:

$$\frac{dF^{(\mathrm{III})}(0)}{dx} = -\frac{dF^{(\mathrm{I})}(0)}{dx}. \tag{44}$$

We show the plot of $dF^{(\mathrm{III})}(0)/dx$ as a function of G_{syn} for several fixed values of β in Fig. 2(c). We see that except for very small β, the stability condition Eq. (42) is satisfied with $dF^{(\mathrm{III})}/(0)dx<1$ for every $G_{syn}>0$. It is noted that the two neurons are attracted to the in-phase synchronized solution with alternating the firing order. However, for $\beta \gtrsim 0.0004$, $dF^{(\mathrm{III})(0)}/dx$ can increase beyond 1 and break down the stability condition of Eq. (43) for a certain interval of G_{syn}. Then in the black region of Fig. 2(b), the in-phase synchronized solution is unstable. In addition, the quasi-in-phase synchronized solution emerges, corresponding to the stable fixed point solution for $x=F^{(\mathrm{III})}\circ F^{(\mathrm{III})}(x)$ given by $x \neq 0$.

B. Antiphase synchronization

There can be several temporal firing patterns leading to antiphase synchronization of the two coupled neurons. The simplest and most important case will be given by Table I: supposing both the two neurons to be inactive, one neuron that expects to fire earlier can stop firing to become inactive before the other neuron starts to fire. We consider an initial condition (nth iterate) as the following:

$$W_1^{--}(0)=W_1^{+-}(0)\equiv W_1^{(n)}+G_{syn}s_2^{(n)},$$

TABLE I. Time evolution of neurons 1 and 2 in the case of antiphase synchronization. The number of the case is in Sec. II. "+" and "-" indicate that each neuron is in the active phase and silent phase.

Duration	Case	Neuron 1	Neuron 2
$[0,\Delta_1]$	2	+	−
$[\Delta_1,t_2]$	3	−	−
$[t_2,t_2+\Delta_2]$	2	−	+
$[t_2+\Delta_2,\Delta_1+\Delta_1']$	3	−	−

$$W_2^{--}(0)=W_2^{-+}(0)\equiv W_2^{(n)},$$

$$s_1^{+}(0)\equiv s_1^{(n)},$$

$$s_2^{-}(0)\equiv s_2^{(n)},$$

where time (0) is set to be the one immediately after neuron 1 fires and hence the initial state of neuron 1 is $W_1^{(n)}=-(2-c)$ and $s_1^{(n)}=1$. We calculate the time evolution of Table I in the same manner as in the above Sec. III A.

Suppose that during time interval $[0,\Delta_1]$, neuron 2 is silent while neuron 1 keeps firing. At $t=\Delta_1$, neuron 1, arriving at the right knee of the V_1 nullcline that is vertically shifted by $G_{syn}s_2(\Delta_1)$, stops firing to jump down to the inactive phase. Here Δ_1 is the time duration of neuron 1's action potential. Then it follows that

$$W_1^{+-}(\Delta_1)=W_1^{--}(\Delta_1)=(2-c)+G_{syn}s_2^{-}(0)e^{-\beta\Delta_1}.$$

Similarly, suppose that for $[\Delta_1,t_2]$, both the two neurons are in the silent phase. At $t=t_2$, neuron 2 begins to fire when it is at the left knee of V_2 nullcline that is vertically shifted by $G_{syn}s_1(t_2)$. The equations representing the state of neuron 2 are then given by

$$W_2^{--}(t_2)=W_2^{+}(t_2)$$
$$=-(2-c)+G_{syn}s_1^{-}(t_1+\Delta_1)e^{-\beta(t_2-\Delta_1)},$$

$$s_2^{-}(t_2)\rightarrow s_2^{+}(t_2)=1.$$

We next assume that for $[t_2,t_2+\Delta_2]$, neuron 1 is in the silent phase but neuron 2 is in the active phase. At $t=t_2+\Delta_2$, neuron 2 stops firing to jump down to the silent phase and is at the right knee of V_2 nullcline that is vertically shifted by $G_{syn}s_1(t_2+\Delta_2)$. Here Δ_2 is the time duration of neuron 2's action potential. Then it follows that

$$W_2^{+-}(t_2+\Delta_2)=W_2^{--}(t_2+\Delta_2)$$
$$=(2-c)+G_{syn}s_1^{-}(t_2)e^{-\beta\Delta_2}.$$

Suppose finally that for $[t_2+\Delta_2,\Delta_1+\Delta_1']$, two neurons are in the silent phase. At $t=\Delta_1+\Delta_1'$, neuron 1 begins to fire again and is at the left knee of V_1 nullcline that is vertically shifted by $G_{syn}s_2(\Delta_1+\Delta_1')$. We obtain the state of neuron 1 as follows:

$$W_1^{--}(\Delta_1+\Delta_1')=W_1^{+-}(\Delta_1+\Delta_1')$$
$$=-(2-c)+G_{syn}s_2^{-}(t_2+\Delta_2)$$
$$\times e^{-\beta(\Delta_1+\Delta_1'-\Delta_2-t_2)},$$

$$s_1^{-}(\Delta_1+\Delta_1')\rightarrow s_1^{+}(\Delta_1+\Delta_1')=1.$$

We now write down the Poincaré map of the solution to Eqs. (8), (9), and (10) for studying the antiphase synchronization

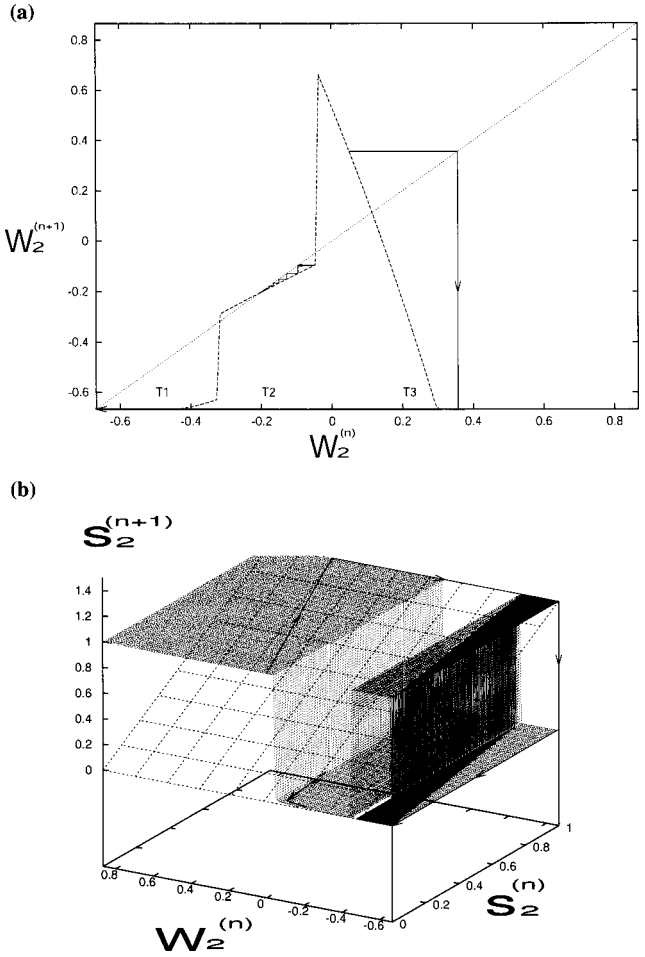

FIG. 3. Whole Poincaré map when β is large (e.g., $\beta=4.5$ and $G_{syn}=0.2$). (a) $W_2^{(n+1)}=F(W_2^{(n)},s_{2,0})$ with $s_{2,0}\approx 0.009$. The dotted line indicates the 45° line. This Poincaré map consists of three branches, $T1$ (Sec. III A), $T2$ (Sec. III B, or Table I), and $T3$ (not shown here). (b) $s_2^{(n+1)}=F(W_2^{(n)},s_2^{(n)})$. The grid plane shows the 45° plane.

$$L(W_2^{(n)},s_2^{(n)})=(W_2^{(n+1)},s_2^{(n+1)})$$
$$=[W_2^{--}(\Delta_1+\Delta_1'),s_2^{-}(\Delta_1+\Delta_1')]. \quad (45)$$

More precisely, we define the antiphase synchronized solution as the fixed point of the above map.

IV. RESULTS AND CONCLUSIONS

The whole Poincaré map $F(W_2^{(n)},s_2^{(n)})$ is defined for $W_2^{(n)}$ in the entire region $[-(2-c),(2-c)+G_{syn}]$ in the case of excitatory coupling (or $[-(2-c)+G_{syn},(2-c)]$ when inhibitory). This map can be obtained by incorporating other temporal firing pattern diagrams as well as the temporal firing pattern diagram of Sec. III A and Table I. An example of the map $F(W_2^{(n)},s_2^{(n)})$ is shown in Figs. 3 and 6. Figures 3(a) and 3(b), respectively, display $W_2^{(n+1)}=F(W_2^{(n)},s_{2,0}^{(n)})$ with $s_{2,0}^{(n)}\approx 0.009$ and $s_2^{(n+1)}=F(W_2^{(n)},s_2^{(n)})$, respectively, for an excitatory coupling. On the other hand, Fig. 6(a) and 6(b) represent $W_2^{(n+1)}=F(W_2^{(n)},s_2^{(n)})$ and $s_2^{(n+1)}=F(W_2^{(n)},s_2^{(n)})$,

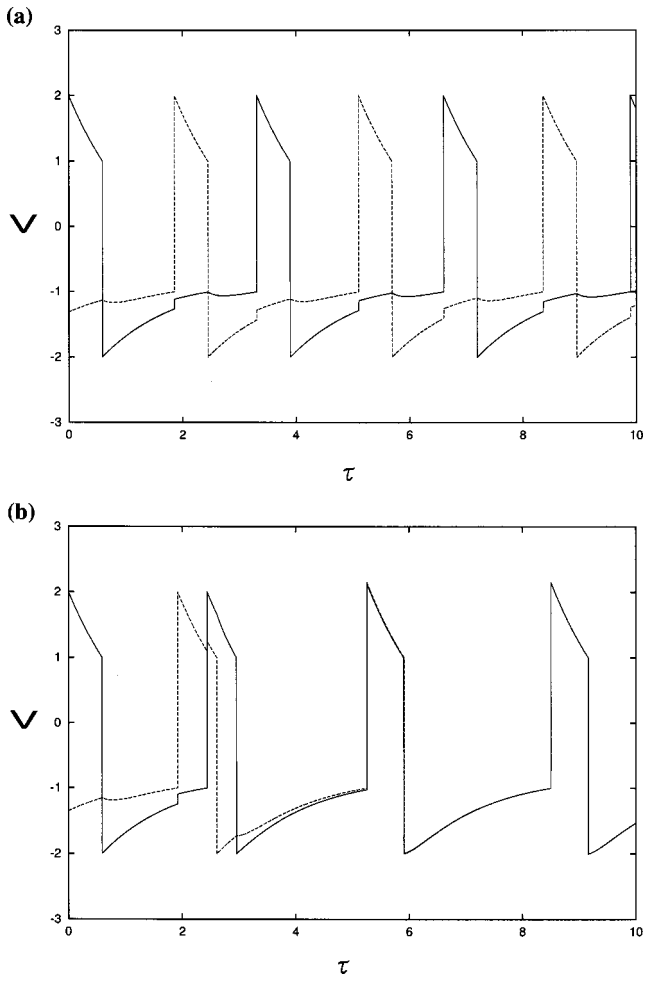

FIG. 4. Synchronization phenomena when β is large. The two neurons become synchronized in (a) the antiphase and (b) the in phase.

respectively, for an inhibitory coupling. On the basis of such Poincaré maps together with the results of the temporal firing pattern diagram in Secs. III A and III B, we deal with in-phase as well as antiphase synchronized solutions together with the transient dynamics setting into them.

Now set $a=0.8, b=0.01, c=\frac{4}{3}, \theta=0.0$. We show the results of the synchronization behavior of our system obtained theoretically and by numerical simulations.

A. Excitatory synaptic coupling

In the case of excitatory synaptic coupling, there occur three types of behavior of synchronization for large times according to the values of G_{syn} and β. When β is large (e.g., $\beta=4.5$) and G_{syn} is small, we have the anti-phase [as shown in Fig. 4(a)] and in-phase [as shown in Fig. 4(b)] synchronized solutions depending on the initial condition. Figure 3 shows a typical whole Poincaré map of the system with such a condition for G_{syn} and β. In Fig. 3, the solid lines with arrows represent trajectories that are obtained from iterations of the map. We see that there exist two fixed points that are given by intersections of the one-dimensional cross section of the whole Poincaré map and the 45° line in Fig. 3(a) [or the two-dimensional map and the 45° plane in Fig. 3(b)]. The fixed point $(-0.667, 0.000)$ of the $T1$ branch represents the in-phase synchronized solution, while the fixed point $(-0.205, 0.009)$ of the $T2$ branch represents the antiphase synchronized solution. Figures 3(a) and 3(b) also show that as time elapses the trajectory of neuron 2's state (started from an arbitrary initial condition) is eventually attracted into either of the two fixed points. Such behavior is shown in Fig. 5: In Fig. 5(a), the blank region represents the in-phase synchronized solution, while the vertical striped region represents the antiphase synchronized solution. Figure 5(b) shows the plot of $|W_2-W_1|$ for large times as a function of β for fixed value of G_{syn}. Figure 5(c) shows the plot of $|W_2-W_1|$ for large times of neuron 2's initial condition $(W_2^{(0)}, s_2^{(0)})$ for fixed values of G_{syn} and β. We then find that the antiphase as well as the in-phase synchronizations are determined by the differing initial state of neuron 2. The in-phase synchronized solution given by the fixed point of $T1$ branch corresponds to the one of region (III) in Fig. 2(a); the occurrence of the alternating firing order of neurons 1 and 2 in approaching the fixed point can be seen by noting the trajectory following a square path in Fig. 3(b). The fact that $s_2^{(n+1)}$ can take 1 implies that neuron 2 can fire earlier than neuron 1 and one has reversal of firing order. If G_{syn} becomes larger than a certain critical value $G_{syn}^{crit}(\beta)$, two neurons are attracted to the fixed point without alternating the firing order. This is shown in regions (I) and (II) in Fig. 2(a).

For (G_{syn}, β) other than the above-mentioned condition, the antiphase synchronized solution disappears. In such a Case, if G_{syn} is larger than a certain critical value G_{syn}^{crit}, only the in-phase synchronized solution remains in existence. The solution demonstrates that although two neurons fire simultaneously, they are attracted to the solution without alternating the firing order. However if $G_{syn}<G_{syn}^{crit}$, two neurons are attracted to the in-phase synchronized solution with alternating the firing order. Here G_{syn}^{crit} is determined by the solid line in Figs. 2(a) and 2(b).

Moreover, as shown in Fig. 2(b), when β is sufficiently smaller (e.g., $\beta=0.0001$), there exists a certain (G_{syn}, β) region that has the following synchronization phenomenon: Although two neurons fire simultaneously, they cannot be attracted to the in-phase solution with $x=0$ but to the nearly in-phase one with a small phase difference $(x\neq 0)$.

B. Inhibitory synaptic coupling

When β is small(e.g., $\beta=0.001$), the whole Poincaré map for the case with inhibitory synaptic coupling gives only one stable fixed point in Table I. The trajectory started from an arbitrary initial state of neuron 2 is attracted to the fixed point. It represents the antiphase synchronized solution, which is shown in Fig. 6.

However, when β becomes larger than the critical value, the whole Poincaré map yields a pair of stable fixed points in Table I. The pair arises from the occurrence of bifurcation at the critical value of β. This map is demonstrated in Figs. 7(a) and 7(b). Figures 7(a) and 7(b) show $W_2^{(n+1)}$

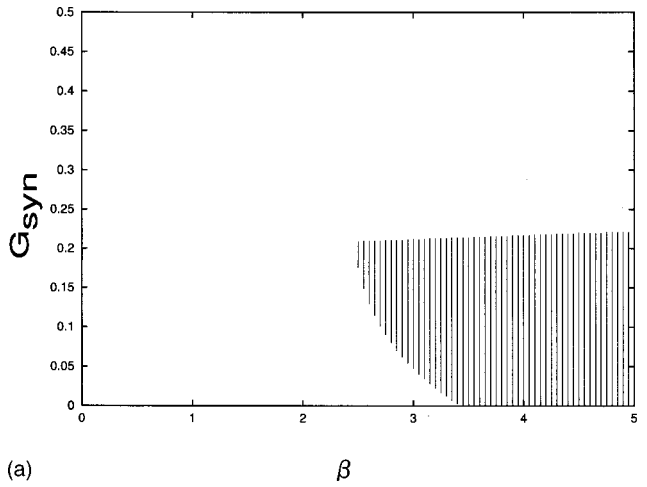

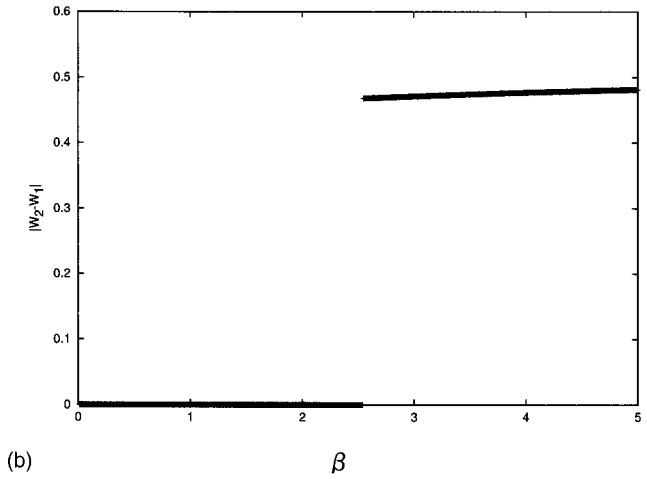

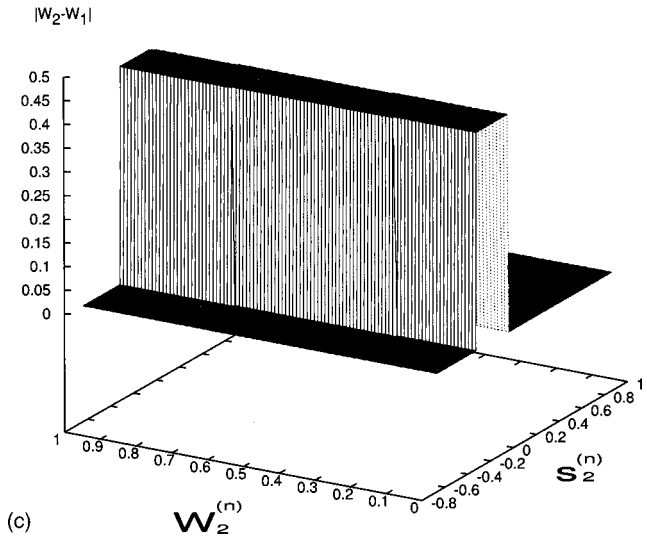

FIG. 5. Phase diagrams concerning the in-phase and antiphase synchronizations with excitatory coupling when the initial state of neuron 2 is $W_2^{(n)}=-0.25$ and $s_2^{(n)}=0.0$. (a) $\beta-G_{syn}$ diagram. (b) β-$|W_1-W_2|$ diagram for $G_{syn}=0.2$. (c) Neuron 2's initial state and $|W_2-W_1|$ diagram when $G_{syn}=0.2$ and $\beta=4.5$.

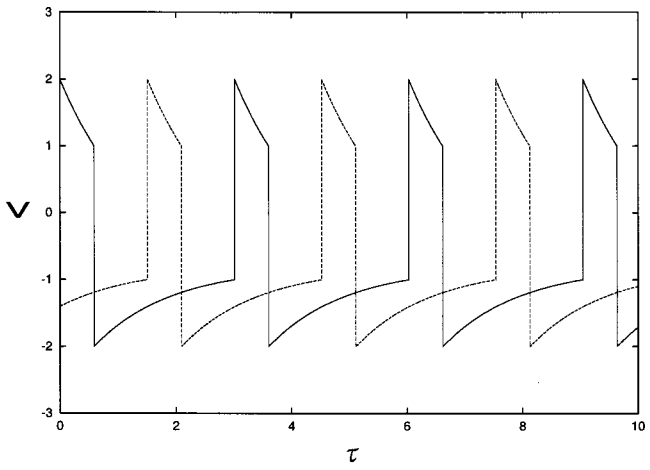

FIG. 6. Synchronization phenomena when β is small. The two neurons become synchronized in the antiphase.

$=F(W_2^{(n)},s_2^{(n)})$ and $s_2^{(n+1)}=F(W_2^{(n)},s_2^{(n)})$, respectively. The pair of stable fixed points represent a kind of antiphase synchronized solution. Such synchronized solutions, however, may happen to be viewed as a kind of in-phase synchronized

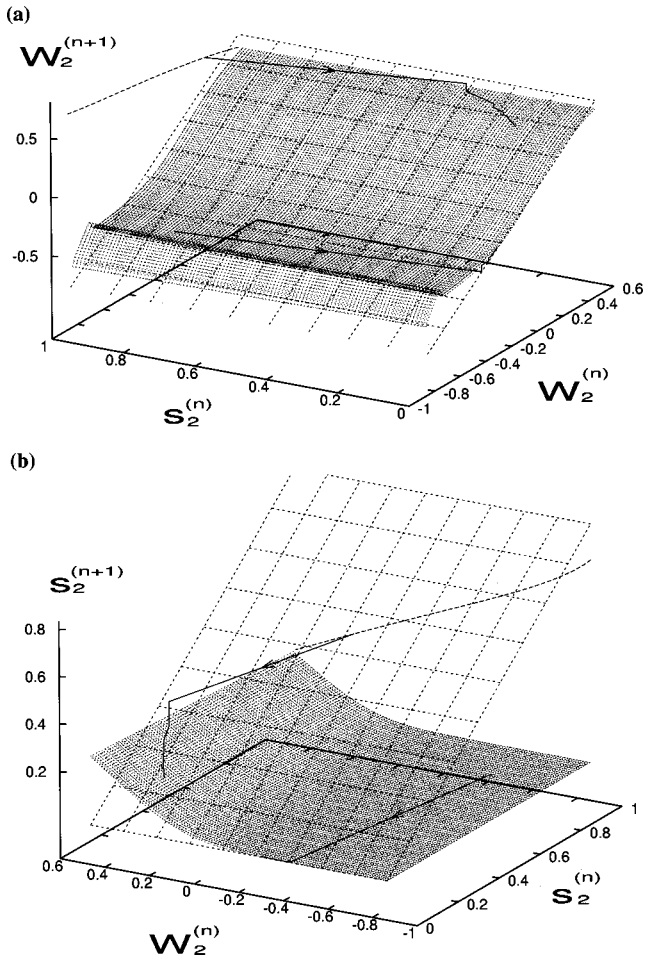

FIG. 7. Two-dimensional Poincaré map when β is large (e.g., $\beta=5.0$ and $G_{syn}=-0.2$). (a) $W_2^{(n+1)}=F(W_2^{(n)},s_2^{(n)})$. (b) $s_2^{(n+1)}=F(W_2^{(n)},s_2^{(n)})$.

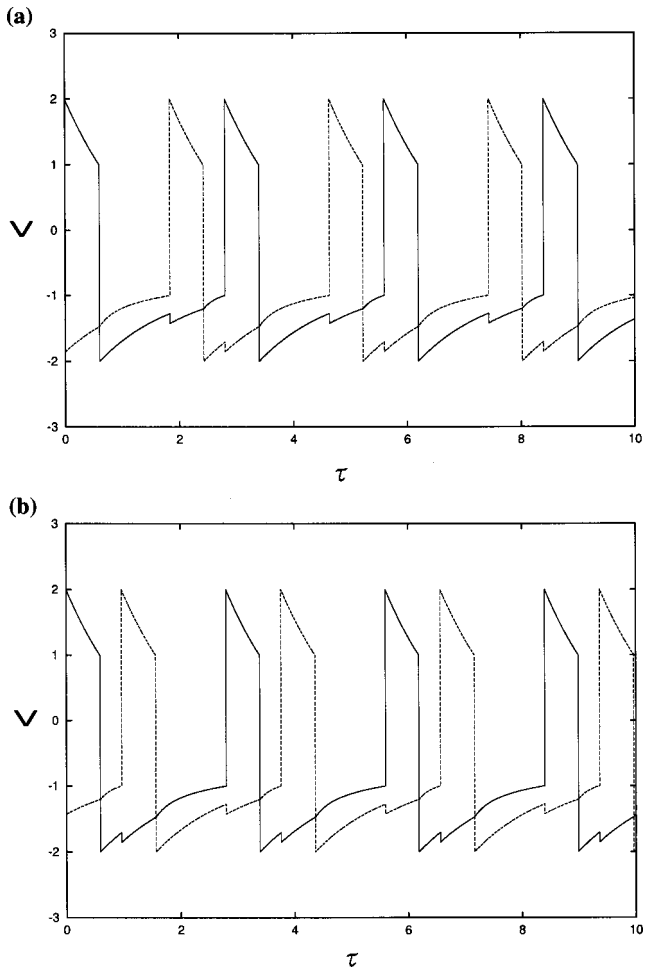

FIG. 8. Synchronization phenomena when β is large. In both (a) and (b), the two neurons become synchronized with a short phase interval. Neuron 2's initial configuration replaces neuron 1's firing order with that of neuron 2.

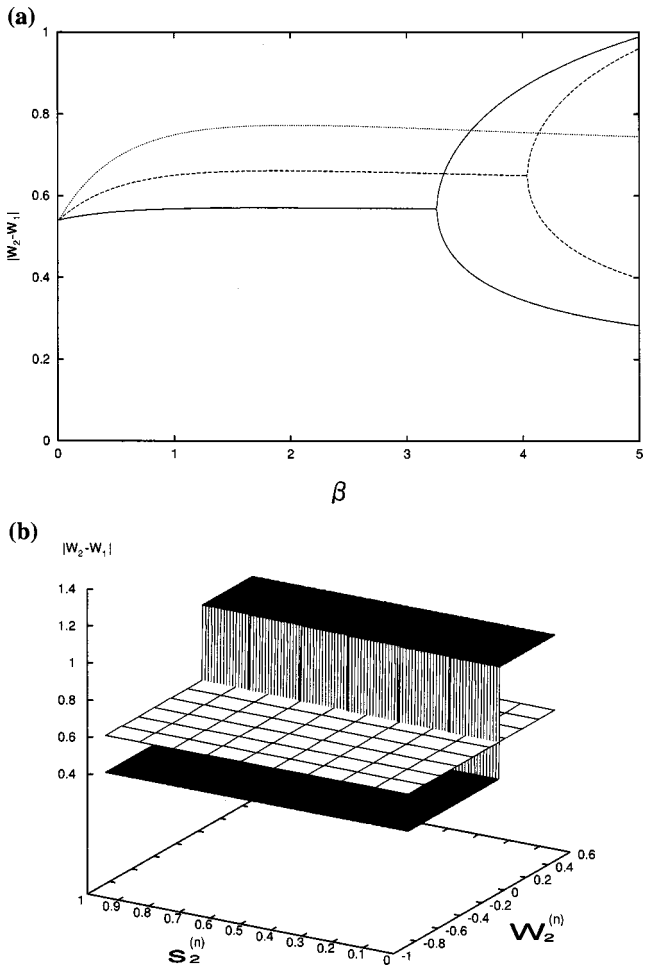

FIG. 9. Phase diagram in inhibitory coupling when the initial state of neuron 2 is $W_2^{(n)}=-0.25$ and $s_2^{(n)}=0.0$. (a) β-$|W_2-W_1|$ diagram due to the differing level of G_{syn}: the solid, dotted, and broken lines are shown when $G_{syn}=-0.06$, -0.24, and -0.46, respectively. (b) Neuron 2's initial state and $|W_2-W_1|$ diagram due to the differing level of β. The solid plane when $\beta=5.0$ and $G_{syn}=-0.2$. The grid plane when $\beta=0.1$ and $G_{syn}=-0.3$.

solution because two neurons become synchronized at a short intervals. This phenomenon is demonstrated in Figs. 8(a) and 8(b). We call this type of synchronized solution the quasiantiphase synchronized solution. We then find that neuron 2's initial configuration replaces neuron 1's firing order with that of neuron 2.

As a result, the above conclusion is shown in Figs. 9(a) and 9(b). Figure 9(a) indicates the plot of the phase difference of neurons 1 and 2 as $t\rightarrow\infty$ as a function of β for several fixed values of G_{syn}. As β becomes larger to pass through a critical value of β, the two neurons switch from antiphase to quasiantiphase synchronization. Figure 9(b) shows such a behavior: when β is large (e.g., $\beta=5.0$ and $G_{syn}=-0.2$), $|W_2-W_1|$ depends on the initial state of neuron 2 and is separated by it. However, if β is small (e.g., $\beta=0.1$ and $G_{syn}=-0.3$), the phase difference is constant, and independent from the initial state.

V. SUMMARY AND DISCUSSION

Our analysis is based on the construction of the Poincaré map for the dynamics of the coupled piecewise-linear model neurons. The analysis has enabled us to explain the in-phase or antiphase synchronizations exhibited by a pair of synaptically interconnected neurons in a concrete and systematic manner. In addition to the commonly known in-phase and antiphase synchronizations, we have found the occurrences of quasi-in-phase and quasiantiphase synchronization. These phenomena, to the best of our knowledge, have not been reported or studied so far. In the case of excitatory coupling, when the decaying relaxation rate is large, two neurons get synchronized in the in phase or antiphase depending on initial conditions for neurons. However, if it is small, they become synchronized in the in phase. On the other hand, in the case of inhibitory coupling, if the decaying relaxation rate is small, the neurons become synchronized in the antiphase. However, as it becomes larger than the critical value of β, they become synchronized in the quasiantiphase.

Moreover, we have had a clear view of the behavior of transient dynamics setting into the in-phase synchronized state. In this study, there occur two types of firing patterns

with respect to firing order. We obtained the boundary line between the two transient firing patterns in the phase diagram of G_{syn} and β.

Our theoretical results indicate that excitation rather than inhibition produces synchrony when synaptic response due to activation of neurons occurs instantaneously and decays very slowly. This should be contrasted with the result of previous work based on theoretical and simulation based studies: Inhibition rather than excitation was reported to produce synchrony in the case when synaptic rising times are larger than the width of an action potential. In this study, we neglected to take into account the effect of the synaptic rising time by assuming, for the sake of simplicity, that the synaptic rising time is sufficiently small.

In spite of the analysis based on taking the limit $\epsilon \to 0$, our results agree with those of numerical simulations for the original Eqs. (1) and (2) with small ϵ. Furthermore, they are also qualitatively in agreement with the result of numerical simulations for the HH model with small ϵ ($\epsilon = 0.05$). This implies the validity of our approach of taking $\epsilon \to 0$ limit and of using piecewise-linear model for investigating the synchronization phenomena of two coupled neurons. On the other hand, when ϵ becomes large, in the present piecewise-linear model, we have found by numerical simulations that the in-phase synchronization occurs in the two inhibitory synaptic coupled neurons. The occurrence of such phenomena (inhibitory synchrony) was also reported by Wang and Buzsáki [12] for the HH model which had extremely rapid rising and slowly decaying synaptic response times. Excitatory and inhibitory synaptic couplings lead to asynchronization, and synchronization in the in phase or antiphase, respectively.

Therefore, the key feature that determines which of in-phase and antiphase synchronized firings occurs in coupled neurons with synaptic interaction depends crucially on the rising time of the synaptic response and ϵ. Accordingly, we will have to investigate the synchronization phenomena, including in the large ϵ.

APPENDIX A: LINEAR ANALYSIS OF THE FIRING TIME DIFFERENCE OF NEURONS NEAR THE LEFT KNEE POINT

We investigate the condition for the occurrence of the case where neuron 2 arrives at the knee point earlier than neuron 1.

We analyze the state of neuron 1 (or neuron 2) at the left knee point in phase plane, supposing Δ_1 to be infinitesimally small $\Delta_1 = \delta s_1$, we set $\Delta_2 = T_2 + \delta s_2$ (or $\Delta_2 = T_2 + \delta s_2'$). where it takes T_2 for two neurons to jump down simultaneously to the inactive phase and enter simultaneously into the active phase. Considering the moment when neuron 1 arrives at the left knee point of V nullcline, we have

$$\begin{aligned} &-(2-c) + G_{syn} e^{-\beta(T_2+\delta s_2)} \\ &\quad = \{[(2-c) - G_{syn} - D_-] e^{-[b+(1/c)]\delta s_1} - D_- - A_- - B\} \\ &\qquad \times e^{-[b+(1/c)](T_2+\delta s_2)} + B e^{-\beta(T_2+\delta s_2)} + A_- . \end{aligned} \tag{A1}$$

Up to the first order in δs_1 and δs_2, we obtain δs_2:

$$\delta s_2 = \frac{\left(b + \frac{1}{c}\right)[(2-c) - G_{syn} - D_-] e^{-[b+(1/c)]T_2}}{-\left(b + \frac{1}{c}\right)[(2-c) + (G_{syn} - B) - A_-] e^{-[b+(1/c)]T_2} - \beta(B - G_{syn}) e^{-\beta T_2}} \delta s_1 . \tag{A2}$$

Similarly, suppose that neuron 2 arrives at the left knee point. Using the aforementioned analysis, we obtain $\delta s_2'$:

$$\delta s_2' = \frac{\beta(B - G_{syn})(e^{-\beta T_2} - e^{-[b+(1/c)]T_2})}{-[b+(1/c)][(2-c) + (G_{syn} - B) - A_-] e^{-[b+(1/c)]T_2} - \beta(B - G_{syn}) e^{-\beta T_2}} \delta s_1 . \tag{A3}$$

By $\delta s_2 - \delta s_2'$, we can determine which of neurons 1 and 2 arrives earlier at the left knee point. Then the broken line in Fig. 2(a) which corresponds to $\delta s_2 - \delta s_2' = 0$, gives us the resulting equation:

$$\begin{aligned} &\left(b + \frac{1}{c}\right)[(2-c) + G_{syn} - D_-] e^{-[b+(1/c)]T_2} - \beta(G_{syn} - B) \\ &\qquad \times (e^{-\beta T_2} - e^{-[b+(1/c)]T_2}) = 0. \end{aligned} \tag{A4}$$

In Fig. 2(a), region (I) indicates that neuron 2 reaches the left knee earlier than neuron 1 ($\delta s_2 - \delta s_2' > 0$), whereas regions (II) and (III) demonstrate that neuron 1 arrives at the left knee earlier than neuron 2 ($\delta s_2 - \delta s_2' < 0$).

APPENDIX B: POINCARÉ MAPS FOR IN-PHASE SYNCHRONIZATION

According to inequality $\delta s_2 - \delta s_2' > (\text{or} <)\ 0$ and $W_1^{--}(\Delta_1 + \Delta_2) > (\text{or} <)\ W_2^{--}(\Delta_1 + \Delta_2)$ [see Eq. (30)], we have three cases of temporal firing pattern diagrams based on which the corresponding Poincaré map can be constructed. The three cases are displayed as (I), (II), and (III) in the phase diagram of Fig. 2(a).

Region (I). $\delta s_2 - \delta s_2' > 0$ and $W_1^{--}(\Delta_1+\Delta_2) > W_2^{--}(\Delta_1+\Delta_2)$. Using Eqs. (24), (25), (26), (31), and (37), we have the return map from Eq. (40)

$$F^{(\mathrm{I})}(x) = [(2-c)+G_{syn}-D_+]\left(1-\frac{h_1(\Delta_1,\Delta_2)}{h_2(\Delta_1,\Delta_2)}\right),$$

$$h_1(\Delta_1,\Delta_2) = \{[(2-c)+G_{syn}-D_-]e^{-[b+(1/c)]\Delta_1} + D_+ - A_- - B\}e^{-[b+(1/c)]\Delta_2} + Be^{-\beta\Delta_2} + A_-,$$

$$h_2(\Delta_1,\Delta_2) = -(2-c)+G_{syn}e^{-\beta(\Delta_2+\Delta_1)}, \qquad \text{(B1)}$$

where $\Delta_1(x)$ and $\Delta_2(\Delta_1)$ satisfy the following equations:

$$[(2-c)-A_+]+(G_{syn}-B)e^{-\beta\Delta_1} - [(2-c)+G_{syn}-x-A_+-B]e^{-[b+(1/c)]\Delta_1}=0, \qquad \text{(B2)}$$

$$[-(2-c)-A_-]+(G_{syn}-B)e^{-\beta(\Delta_1+\Delta_2)} - [(2-c)-A_-+(G_{syn}-B)e^{-\beta\Delta_1}]e^{-[b+(1/c)]\Delta_2}=0. \qquad \text{(B3)}$$

Region (II). $\delta s_2 - \delta s_2' < 0$ and $W_1^{--}(\Delta_1+\Delta_2) > W_2^{--}(\Delta_1+\Delta_2)$. We have

$$F^{(\mathrm{II})}(x) = [(2-c)+G_{syn}-D_+]\left(1-\frac{g_2(\Delta_1,\Delta_2)}{g_1(\Delta_1,\Delta_2)}\right). \qquad \text{(B4)}$$

Region (III). $\delta s_2 - \delta s_2' < 0$ and $W_1^{--}(\Delta_1+\Delta_2) < W_2^{--}(\Delta_1+\Delta_2)$. We obtain

$$F^{(\mathrm{III})}(x) = [(2-c)+G_{syn}-D_+]\left(1-\frac{g_1(\Delta_1,\Delta_2)}{g_2(\Delta_1,\Delta_2)}\right), \qquad \text{(B5)}$$

$$g_1(\Delta_1,\Delta_2) = -(2-c)+G_{syn}e^{-\beta\Delta_2},$$

$$g_2(\Delta_1,\Delta_2) = [(2-c)+(G_{syn}-B)e^{-\beta\Delta_1}-A_-]e^{-[b+(1/c)]\Delta_2} + Be^{-\beta(\Delta_1+\Delta_2)}+A_-,$$

where $\Delta_1(x)$ and $\Delta_2(\Delta_1)$, respectively, satisfy Eq. (B2) and the following equation:

$$[-(2-c)-A_-]+(G_{syn}-B)e^{-\beta\Delta_2} - [(2-c)+G_{syn}-D_-]e^{-[b+(1/c)]\Delta_1} + (D_- - A_- - B)e^{-[b+(1/c)]\Delta_2}=0. \qquad \text{(B6)}$$

To conduct linear stability analysis of $x_{n+1}=F^{(\mathrm{I})}(x_n)$, we calculate the derivation of $F^{(\mathrm{I})}(x_n)$ at $x=0$,

$$\left.\frac{dF^{(\mathrm{I})}}{dx}\right|_{x=0} = \left(\frac{\partial F^{(\mathrm{I})}}{\partial\Delta_1}+\frac{\partial F^{(\mathrm{I})}}{\partial\Delta_2}\frac{d\Delta_2}{d\Delta_1}\right)\left.\frac{d\Delta_1}{dx}\right|_{\Delta_1=0,\Delta_2=T_2}. \qquad \text{(B7)}$$

Using Eq. (B3), T_2 satisfies

$$[-(2-c)-A_-]+(G_{syn}-B)e^{-\beta T_2} - [(2-c)-A_-+G_{syn}-B]e^{-[b+(1/c)]T_2}=0. \qquad \text{(B8)}$$

It then follows that Eq. (41) holds. Similarly, from Eq. (B8), we obtain Eq. (44). Furthermore, the phase boundary between the phases of (II) and (III), which is defined by $W_1^{--}(\Delta_1+\Delta_2)=W_2^{--}(\Delta_1+\Delta_2)$ with infinitesimally small Δ_1, turns out to be given by $dF^{(\mathrm{I})}/dx|_{x=0}=0$

$$\left(b+\frac{1}{c}\right)[(2-c)+G_{syn}-D_-]e^{-[b+(1/c)]T_2} - \beta[(G_{syn}-B)e^{-[b+(1/c)]T_2}+Be^{-\beta T_2}]=0. \qquad \text{(B9)}$$

[1] C.M. Gray and W. Singer, Proc. Natl. Acad. Sci. U.S.A. **86**, 1698 (1989).
[2] C.M. Gray, P. König, A.K. Engel, and W. Singer, Nature (London) **338**, 334 (1989).
[3] A.K. Engel, P. König, and W. Singer, Proc. Natl. Acad. Sci. U.S.A. **88**, 9136 (1991).
[4] P. Fries, P.R. Roelfsema, A.K. Engel, P. König, and W. Singer, Proc. Natl. Acad. Sci. U.S.A. **94**, 12699 (1997).
[5] H. Golomb, D. Hansel, B. Shraiman, and H. Sompolinsky, Phys. Rev. A **45**, 3516 (1992).
[6] D. Hansel, G. Mato, and C. Meunier, Phys. Rev. E **48**, 3470 (1993).
[7] D. Hansel, G. Mato, and C. Meunier, Neural Comput. **7**, 307 (1995).
[8] K. Okuda, Physica D **63**, 424 (1993).
[9] R.C. Elson, A.I. Selverston, R. Huerta, N.F. Rulkov, M.I. Rabinovich, and H.D.I. Abarbanel, Phys. Rev. Lett. **81**, 5692 (1998).
[10] R. Herrero, M. Figueras, J. Rius, F. Pi, and G. Orriols, Phys. Rev. Lett. **84**, 5312 (2000).
[11] R.D. Pinto, P. Varona, A.R. Volkovskii, A. Szües, H.D.I. Abarbanel, and M.I. Rabinovich, Phys. Rev. E **62**, 2644 (2000).
[12] X.J. Wang and G. Buzsáki, J. Neurosci. **16**, 6402 (1996).
[13] X.J. Wang and J. Rinzel, Neural Comput. **4**, 84 (1992).
[14] X.J. Wang and J. Rinzel, Neuroscience **53**, 899 (1993).
[15] D. Golomb, X.J. Wang, and J. Rinzel, J. Neurophysiol. **72**, 1109 (1994).
[16] C. Van Vreeswijk, L.M. Abbott, and G.B. Ermentrout, J. Comput. Neurosci. **1**, 1313 (1994).
[17] S. Kim, H. Kook, S.G. Lee, and H.M. Park, Int. J. Bifurcation Chaos Appl. Sci. Eng. **8**, 731 (1998).
[18] S. Kim, H. Kook, and J.H. Shin, *The Statistical Mechanics Perspective*, edited by J.H. Oh, C. Kown, and S. Cho (World Scientific, Singapore, 1995), p. 141.
[19] S.G. Lee, S. Kim, and H. Kook, Int. J. Bifurcation Chaos Appl. Sci. Eng. **7**, 889 (1997).

[20] T. Yoshinaga, Y. Sano, and H. Kawakami, Int. J. Bifurcation Chaos Appl. Sci. Eng. **9**, 1451 (1999).
[21] K. Tsumoto, T. Yoshinaga, and H. Kawakami, Int. J. Bifurcation and Chaos (to be published).
[22] G. Renversez, Physica D **114**, 114 (1998).
[23] D. Somers and N. Kopell, Biol. Cybern. **68**, 393 (1993).
[24] T. Ohta, A. Ito, and A. Tetsuka, Phys. Rev. A **42**, 3225 (1990).
[25] T. Ohta and H. Nakazawa, Phys. Rev. A **45**, 5504 (1992).
[26] R. Kobayashi, T. Ohta, and Y. Hayase, Phys. Rev. E **50**, R3291 (1994).
[27] D. Ruwisch *et al.*, Int. J. Bifurcation Chaos Appl. Sci. Eng. **9**, 1969 (1999).
[28] D. Terman and D.L. Wang, Physica D **81**, 148 (1995).
[29] D. Terman and E. Lee, SIAM (Soc. Ind. Appl. Math.) J. Appl. Math. **57**, 252 (1997).
[30] D. Terman, N. Kopell, and A. Bose, Physica D **117**, 241 (1998).
[31] S.R. Campbell and D.L. Wang, Physica D **111**, 151 (1998).
[32] D.L. Wang, *Wiley Encyclopedia of Electrical and Electronics Engineering*, edited by J.G. Webster (Wiley, New York, 1999), p. 396.
[33] A. Bose, V. Booth, and M. Recce, J. Comput. Neurosci. **9**, 5 (2000).